ACS OMEGA

http://pubs.acs.org/journal/acsodf

Article

Advancing Graphene Imaging for Clear Identification of Lattice Defects: The Application of Revolve Sphere Levelling to Scanning Tunnelling Microscopy Images

Disha Bandyopadhyay,* Yiwei Sun,* Ross Griffin, and Lok Yi Lee

Cite This: *ACS Omega* 2024, 9, 43447–43452

Read Online

ACCESS | Metrics & More | Article Recommendations | Supporting Information

ABSTRACT: Application of revolve sphere levelling (RSL) as a practical and effective image processing tool for enhancing scanning tunnelling microscopy (STM) images of graphene atomic lattices is presented. Low-cost, ambient, and non-invasive STM methods overcome limitations of traditional imaging methods like scanning transmission electron microscopy (STEM) and transmission electron microscopy (TEM) that can introduce or alter defects in graphene. Utilizing high-quality graphene synthesized via Paragraf's patented Metal-Organic Chemical Vapor Deposition (MOCVD) method, RSL, which is easily implemented via the Gwyddion software package, effectively highlights the hexagonal lattice structure and specific defect structures. This provides clarity of the atomic structure that traditional methods struggle to achieve. This research emphasizes the utility of RSL in materials science for defect identification in graphene, and points to future research in optimizing RSL for a broader range of defects and applications in other 2D materials.

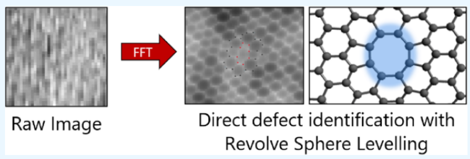

■ INTRODUCTION

Graphene, a two-dimensional material renowned for its unique properties, has attracted significant attention in materials science. Key to its diverse applications are the atomic scale defects present within its lattice, which critically influence its chemical, physical, and electrical properties. These defects, ranging from point to line imperfections, act as scattering centers for electrons and phonons, thereby affecting graphene's optoelectronic performance.[1] Notably, certain defect groups induce local electric and strain fields due to charge redistribution across the lattice. Research by Balasubramanian[2] and Zambudio et al.[3] highlight how defect distribution and monovacancies impact carrier mobility, reactivity, and mechanical properties in graphene. Such insights underscore the importance of defect identification in optimizing graphene's electrical, mechanical, and chemical stability. Further emphasizing this point, Sun et al.[4] demonstrate enhanced stability and charge storage in anode construction using sulfur-rich graphene nanoboxes, a direct result of structural chemical defects.

Traditionally, the atomic lattice structure of graphene has been studied using high-resolution imaging techniques such as high-angle annular dark field (HAADF) imaging mode in scanning transmission electron microscopy (STEM),[5] as well as transmission electron microscopy (TEM).[6] However, these techniques present significant limitations. The sample preparation involves placing the graphene sample on a TEM grid, potentially introducing defects and dislocations in chemical vapor deposition (CVD)-grown graphene. This process, coupled with the need for thin-layer exfoliation and transfer to the TEM grid, can introduce further defects and alter the lattice structure, as explored by Hettler et al.[7] Additionally, these techniques are invasive, with the beam energy needed for high-resolution imaging causing radiation damage.[8]

In light of these challenges, scanning tunneling microscopy (STM) emerges as a viable, noninvasive alternative.[9,10] STM leverages a tunneling current between a probe and the sample surface to glean topography and density of states information. Its advantages include lower operational costs and the ability to function in atmospheric conditions.[11,12]

Additionally, directly interpreting atomic structures, especially defect structures, requires sophisticated image processing and comparison with computer-simulated models.[12] To accurately achieve atomic scale imaging, high vacuum and low temperature systems are typically required.[13] Regardless of the robustness of the experimental set up, sophisticated image processing methods such as Fast Fourier Transforms (FFT) are required to transform the data and compare it to computer simulations of defect structures to evaluate the material.[14−17] Table S1 provides more detail for data collection in the current state of art. The methods rely heavily on postimaging processing and simulations. These multiple image processing steps could introduce errors or biases based on the models used. The inability to directly detect and resolve certain

Received: May 16, 2024
Revised: September 9, 2024
Accepted: September 12, 2024
Published: October 14, 2024

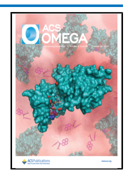

https://doi.org/10.1021/acsomega.4c04675
ACS Omega 2024, 9, 43447–43452

structural features indicates a gap that future technological advancements need to address.

To tackle these challenges, image processing with Revolve Sphere Levelling (RSL) presents an innovative solution to detect lattice edges directly using a singular leveling step. Historically used in gravitational field modeling to process residual disturbance potentials,[18−20] RSL addresses the noise and disturbances inherent in graphene sheets as well as contributions from the environment. These disturbances arise from a multitude of factors including thermal vibrations, edge instabilities, and strain in 2D crystals.[21] By applying RSL as an image processing step, noise and substrate contributions are filtered out, enhancing the visualization of the expected hexagonal lattice structure.

To address the limitation of RSL in processing highly defective graphene images, the use of high-quality graphene synthesized through Paragraf's patented Metal−Organic Chemical Vapor Deposition (MOCVD)[22] approach is beneficial. This method ensures the production of graphene with fewer defects, making it more suitable for effective RSL analysis.

In this paper, RSL as an image processing method is explored to resolve atomic resolution defect structures in graphene. Using an affordable benchtop STM system under atmospheric conditions, we demonstrate the effectiveness of RSL in revealing theoretical defect structures and visualizing the intricate lattice structure of graphene. This advancement in image processing paves the way for a deeper understanding of graphene's defects and their implications in material science and nanotechnology.

■ METHOD

Experimental Section. The STM microscope used for imaging was the Nanosurf NaioSTM system operating in ambient air. Imaging was performed under constant current mode with set point of 1 nA and tip voltage 50.1 mV. The tip was mechanically prepared from a Pt 80%-Ir20% wire. MOCVD grown graphene on sapphire substrates produced by Paragraf's patented technology[22] was imaged.

Samples were prepared by cleaving wafers into squares of sides 1.2 cm. These were attached to STM magnetic stubs with silver paint (AGG3692 electrodag 1415 supplied by Agar scientific) and contacts were painted on with the same silver paint.

Image Processing. The RSL process convolutes a sphere of set radius with the image and subtracts this value as a background style reduction. As the sphere rotates, any irregularities in its levelness will cause the reference point to deviate from a consistent path. By precisely monitoring the deviations and analyzing the collected data, the exact amount and direction of the sphere's nonlevelness can be determined, highlighting the underlying graphene lattice. The methodology and rationale for this type of image processing have been explored by Hartley and Zisserman.[23] A mathematical description about the leveling technique is included in the Supporting Information.

An output of a hexagonal shape characteristic to graphene confirms that this filter can process residual disturbance potentials in the data. Z axis range decreases as the number of the processing steps increases, and therefore, these values become nonphysical for the RSL image in Figure 1c. A consequence of this filtering is a lowered signal-to-noise ratio reducing the STM data from 3D to 2D since the output z scale range decreases post processing.

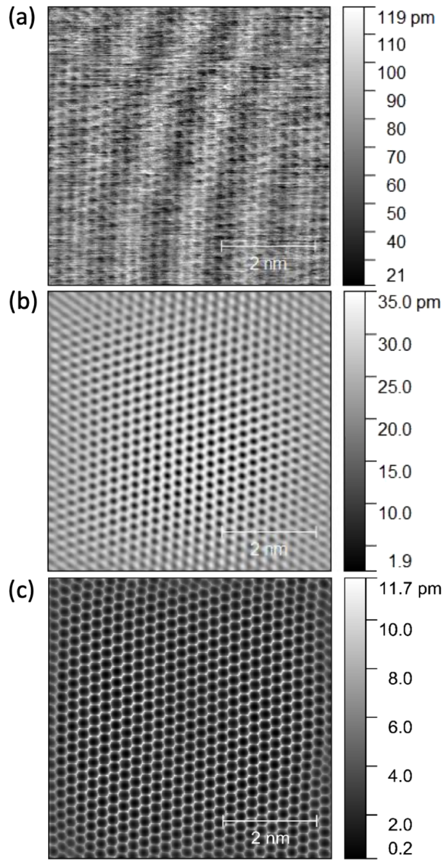

Figure 1. Image processing steps for clear view of individual hexagons within the lattice on Paragraf's synthesized graphene sample. (a) Raw image of pristine graphene. (b) 2D FFT filtered image of (a). (c) RSL applied to (b).

A two-dimensional topographical landscape can be constructed from an STM image. In this landscape, each pixel's height correlates to its brightness in the original STM image. RSL operates by deducting a specific value at each pixel, which is determined by the trajectory of a sphere of a predefined radius as it traverses the landscape derived from the prelevelled image.

The sphere's path is determined by the sphere radius and irregularities in the landscape. As it revolves over the surface, any deviation from a level path is indicative of variations in the surface topology. These deviations are considered background and what remains are considered topographical features of interest, such as the graphene lattice structure.

However, the RSL method is not without limitations. The accuracy of RSL is contingent on the chosen sphere radius; a radius too large overlooks finer details, while a too-small radius overemphasizes minor irregularities. Additionally, RSL assumes a certain degree of uniformity in the landscape, which means it does not perform optimally on images with extreme topographical variations or high levels of noise.

Despite these challenges, RSL's capacity to reveal detailed surface features without complex or expensive equipment makes it a valuable tool in nanoscale material analysis. The principle and effectiveness of this method, as well as its theoretical underpinnings, have been investigated by Hartley,[23] laying a solid foundation for its application in STM image processing.

Raw data was processed using Gwyddion v2.63.[24] Mean plane subtraction was employed to level the surface by eliminating any apparent tilt or shadow effects in the image. Row alignment is critical due to the inherent nature of STM scanning. As the STM probe moves across the surface row by row, it can experience slight tilts or systematic shifts, particularly when transitioning between rows. Aligning the rows compensates for these disturbances, smoothing out inconsistencies across pixels and enhancing the overall image quality.

After completing the initial preparatory steps, we implemented RSL with the sphere's radius set to 0.123 nm.[25] This radius was specifically chosen to correspond with the periodic spacing characteristic of the graphene lattice, namely the distance between the centers of adjacent hexagons. Such precise alignment with the lattice's periodicity enables the RSL algorithm to correct radial distortions in the image. It does this by adjusting areas of the image where these distortions match the sphere's radius, thereby enhancing the visibility of the lattice structure without altering its inherent properties. It is important to note that RSL targets only those distortions that match this set radius; therefore, if the original STM data does not contain radial distortions at this specific scale, the RSL processing will not introduce linear features to flatten the signals at the distortions in the image. Essentially, RSL fine-tunes the image to more accurately represent the graphene's structural details, particularly its hexagonal lattice, by minimizing distortions that are of the same scale as the chosen radius. This also underscores the importance of the radius choice in RSL, as it directly influences the detection and representation of specific structural characteristics in the graphene lattice.

■ RESULTS

In the raw STM image of a pristine graphene sample (Figure 1a), the hexagonal atomic lattice of graphene is recognizable. Application of a 2D FFT filter effectively eliminates low-frequency features, such as the vertical fringes, resulting in a clearer visualization of the lattice, as demonstrated in Figure 1b. The observed blurring in the FFT-processed image edges is attributed to the incomplete lattice (hexagons) at the edge of the raw image. As FFT relies on the periodicity of the image, the break of periodicity of the hexagons at the edges of the raw image not only causes problems in the FFT-processed clearly showing the incomplete hexagons at the edge, but also the surrounding lattice. Subsequently, the implementation of RSL unequivocally reveals individual hexagons within the lattice, as depicted in Figure 1c. It is noteworthy that all images in Figure 1 exhibit the same lattice orientation and an equal number of carbon hexagonal ring structures, indicating that these image processing steps neither introduce nor remove lattice structures.

Figure 2 demonstrates the enhanced clarity of a STEM image of graphene using RSL. Figure 2a presents the FFT-processed and smoothed STEM image from the study by Huang et al.,[12] featuring manually annotated defects that map out the polygonal structures along a grain boundary, annotated by the authors in Figure 2b. The application of RSL to Figure 2a is depicted in Figure 2d, where the lattice structures are brought into sharper contrast, facilitating the precise identification and labeling of polygonal connections at the

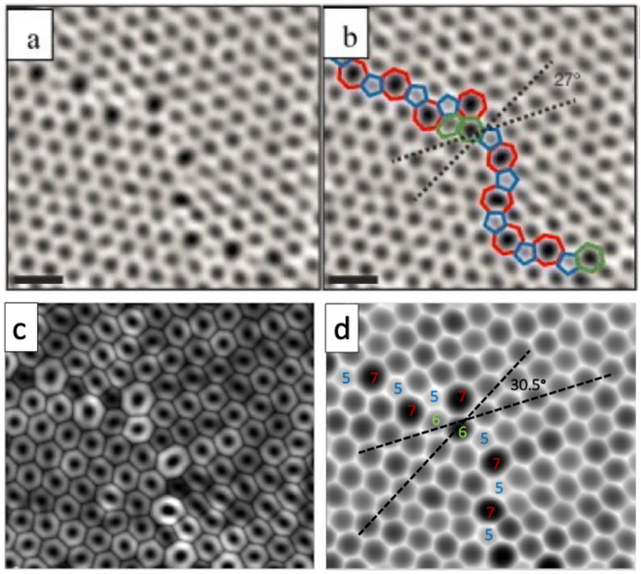

Figure 2. Enhancement of a STEM graphene image from[11] of a graphene grain boundary using Revolving Sphere Levelling (RSL) on image of grain boundary in literature.[12] (a) An FFT-smoothed STEM image of a graphene grain boundary. (b) Manual outlining of polygons along the grain boundary. (c) Image of the superimposition of the RSL-processed image onto (a), illustrating enhanced lattice clarity and the validity of RSL, that it does not create artificial defects. (d) RSL-processed image with labeled polygons at the grain boundary, facilitating a more precise analysis. Both (b) and (d) depict an identical sequence of polygons and present a misorientation angle of the grain boundary that is consistent, validating the RSL method. (a) and (b) from ref 12. The scale bar length is 5 Å. Adapted with permission from Nature[1502270−1]. Copyright [2011] [Nature Research].

grain boundary. This enhanced image clarity allows for a more accurate determination of the grain misorientation angle, measured at 30.5°, which refines the initial estimate of 27° by Huang et al.[12] In Figure 2c, the post-RSL image (Figure 2d) is superimposed onto pre-RSL image (Figure 2a) to confirm the integrity of the lattice features and to demonstrate that RSL does not introduce any artificial elements, as evidenced by the consistent alignment in the superimposition. An estimation of the percentage change in atomic spacing before and after the RSL process has been included in Supporting Information.

Leveraging the enhanced clarity of lattices in Figure 2d, we observe that the polygons comprising the graphene lattice are not equilateral, suggesting variations in the lattice dimensions. Such alterations could signify the presence of stress or strain at the defect sites, or they may be indicative of the polygons being imaged from an oblique perspective. Despite the disruptions at the grain boundary, the graphene atomic lattice elsewhere displays a consistent and uninterrupted pattern.

Graphene is noted for its atomic scale defect structures, often comprising combinations of pentagons, hexagons, heptagons, and octagons.[11] To detect these defects, STM was utilized on Paragraf's graphene samples. STM offers several advantages over STEM in this context: it simplifies operational demands, reduces costs, operates effectively in a variety of environments, minimizes the risk of sample damage due to electron beams, and provides exceptional surface resolution. After acquiring STM images, RSL was applied for image enhancement. This processing step enables clear discernment of the defect structures, as depicted in Table 1.

https://doi.org/10.1021/acsomega.4c04675
ACS Omega 2024, 9, 43447−43452

Table 1. Visualization of Defects in Graphene via RSL-Enhanced STM Imaging[a]

Theoretical simulation of C atom defects	Raw data	FFT processed data	Revolve sphere levelled image
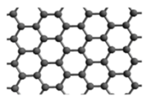 PG	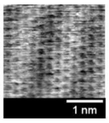	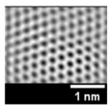	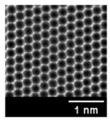
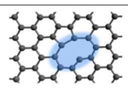 Single vacancy	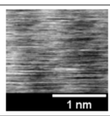	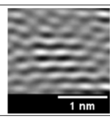	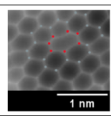
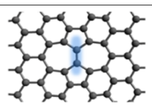 Stone-Wales defect	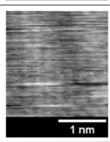	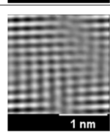	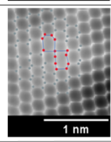
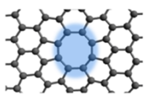 Double vacancy		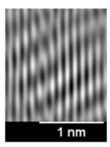	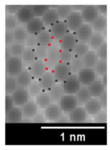

[a]Columns display, from left to right, the simulated atomic lattice structures (adapted from ref 21), the raw data, the initial FFT-processed STM images, and the images post-RSL processing. The rows sequentially represent pristine graphene, and graphene with single vacancy, Stone−Wales, and double vacancy defects. Dots have been manually added for easier identification of defect structures. Red dots in the RSL processed images pinpoint the precise locations of defects, and gray dots indicate the surrounding lattice distortions caused by these defects.

The enhanced image of the double vacancy defect is in agreement with its theoretical simulation,[26] showcasing an octagon flanked by two pentagons and six hexagons. The images of the single vacancy and Stone−Wales defects, while not exact replicas, are close representations of the standard simulations, indicating potential complexities in the simulated models that have not been fully accounted for.

■ DISCUSSION

The introduction of RSL has the potential to overcome many challenges of imaging under ambient conditions, particularly removing the need for high vacuum systems to stabilize STM probe-sample surface interactions for high resolution imaging. With the ability to resolve hexagonal honeycomb lattice structures and identify atomic scale defects under ambient conditions, RSL offers a promising approach to study defect structures in 2D materials.

For the images in Table 1, the match between the FFT data and the RSL-enhanced images is clearest for the pristine graphene (PG) lattice. For the remaining defect structures depicted in Table 1, the defects cannot be identified clearly pre-RSL, as the signal is often significantly obscured by noise. Despite this, the general direction of the underlying lattice remains perceptible and is retained through the filtering process. The RSL technique operates on a straightforward principle: it adjusts the intensity value at each pixel independently, without inducing lateral modifications. Consequently, it is incapable of distorting the lattice imagery or introducing spurious defect structures. This assertion is substantiated by the consistent lattice orientation and the unchanged count of carbon hexagonal ring structures observed in both the pre- and post-RSL images shown in Figure 1. Furthermore, the uniform alignment evident in the super-imposed RSL images of Figure 2 corroborates this conclusion, as discussed in the Results section. Such consistency is crucial, affirming that RSL is a noninvasive image enhancement technique that preserves the intrinsic structural features of the sample.

In assigning the identified defects found in the RSL-processed images specifically to the graphene lattice, we must acknowledge a caveat: STM in principle measures the variations in the Density of States (DoS) near the Fermi level, which it then interprets as topographical features. This technique inherently lacks the ability to differentiate between alterations in electron density due to chemisorption and the intrinsic surface features of the material under investigation.[27] Consequently, what appears as a deviation from the expected eight membered ring structures to seven-membered rings around a single vacancy in Table 1 may not solely represent a topographical defect. It is plausible that this observed irregularity could be attributed to the chemisorption of gases involved in the graphene synthesis process, or as a result of graphene exposing to ambient imaging conditions. This factor demands careful interpretation of STM data, to take chemical alterations of the surface into consideration. We note that there appears to be directional distortion of the graphene lattice in the RSL-processed images. An interpretation could be that there is directional strain in the graphene lattice that it is induced from the combined effect of the slightly anisotropic thermal expansion of the sapphire substrate surface and the defects breaking the in-plane symmetry, resulting in anisotropic adhesion between graphene and sapphire, leading to directional sliding of the graphene.

There are further potential constraints for RSL. Samples characterized by a high degree of disorder or those that are heavily contaminated might not be suitable candidates for RSL analysis, as the technique presupposes a certain degree of symmetry in the raw input image to perform the leveling effectively. Future research should explore the performance of RSL on STM images across a spectrum of sample conditions. This would include analyzing samples with varying levels of disorder and contamination to evaluate the robustness of RSL in these circumstances.

Additionally, the practicality of RSL integration is noteworthy; it can be readily implemented through the Gwyddion software package, which provides a user-friendly platform for STM data analysis. Further studies are required to understand the impact of leveling radius on image processing.

While RSL emerges as the preferred processing technique for our STM images of graphene with the specifically tailored sphere size, it is worth noting that alternative leveling methods, such as median background subtraction and trimmed mean leveling, may also be effective for detecting lattice defects in graphene and other 2D materials. Future research should consider the optimization of kernel sizes for each leveling method across different experimental conditions and strive to develop novel approaches for analyzing larger surface areas and more complicated structures. This progression from simulation to enhanced imaging elucidates the defect structures within the graphene lattice.

In practical applications, precise defects identification in graphene can lead to optimized electronic and optoelectronic devices. The exploration of RSL, particularly through the

https://doi.org/10.1021/acsomega.4c04675
ACS Omega 2024, 9, 43447−43452

Gwyddion software's module, is essential for harnessing the full capabilities of RSL in the analysis of graphene and other two-dimensional materials. We further applied RSL to a recently published image of monolayer MoS2/WS2 to demonstrate its power in identifying atomic defects in general 2D materials, as detailed in the Supporting Information.[28] We acknowledge that the ability of RSL to distinguish defects located in different atomic layers depends on defect density and the resulting lattice spacing variations.[29] Further investigation is needed to confirm this capability. Future research will be instrumental in establishing RSL as a fundamental image processing method for materials characterization.

■ CONCLUSION

This study demonstrates the effectiveness of RSL in processing and elucidating atomic-scale images of monolayer graphene on substrates. These findings significantly contribute to the field of surface profilometry, particularly in STM applications. Our method, using RSL on benchtop STM data, is more accessible and versatile than conventional techniques, which often require expensive equipment and stringent conditions. This advancement not only resolves the hexagonal lattice structure of graphene and identifies defects but also reduces costs and complexity. This enables broader applications in 2D materials research and industry, including the manufacturing of next-generation graphene devices. Moreover, applying RSL to other materials with intricate atomic arrangements will further validate its utility as a versatile data processing technique in material science.

■ ASSOCIATED CONTENT

Supporting Information

The Supporting Information is available free of charge at https://pubs.acs.org/doi/10.1021/acsomega.4c04675.

> Comparative study of STM efforts in literature—S3, estimation of percentage change in atomic spacing before and after RSL process—S4, application of RSL on an image of monolayer MoS_2/WS_2—S5, and revolving sphere levelling (RSL) method—S7 (PDF)

■ AUTHOR INFORMATION

Corresponding Authors

Disha Bandyopadhyay − *Paragraf, Somersham, Huntingdon PE28 3EB, United Kingdom; Ecole Polytechnique Fédérale de Lausanne, Neuchâtel CH-2000, Switzerland;* orcid.org/0000-0002-5444-3451; Email: disha.bandyopadhyay@epfl.ch

Yiwei Sun − *Paragraf, Somersham, Huntingdon PE28 3EB, United Kingdom;* orcid.org/0000-0002-1259-5131; Email: y.sun@paragraf.com

Authors

Ross Griffin − *Paragraf, Somersham, Huntingdon PE28 3EB, United Kingdom; Rutherford Appleton Laboratory, Nium, Didcot OX11 0FA, Oxfordshire*

Lok Yi Lee − *Paragraf, Somersham, Huntingdon PE28 3EB, United Kingdom*

Complete contact information is available at: https://pubs.acs.org/10.1021/acsomega.4c04675

Notes

The authors declare no competing financial interest.

■ ACKNOWLEDGMENTS

The authors thank Dr David Necas from Bruno University of Technology for their help and expertise in understanding RSL for application to STM.

■ REFERENCES

(1) Lewandowska-Andralojc, A.; et al. Understanding structure−properties relationships of porphyrin linked to graphene oxide through π−π-stacking or covalent amide bonds. *Sci. Rep.* **2022**, *12* (1), 13420.

(2) Balasubramanian, K.; et al. Reversible defect engineering in graphene grain boundaries. *Nat. Commun.* **2019**, *10* (1), 1090.

(3) Zambudio, A.; Gnecco, E.; Colchero, J.; Pérez, R.; Gómez-Herrero, J.; Gómez-Navarro, C. Fine defect engineering of graphene friction. *Carbon* **2021**, *182*, 735−741.

(4) Sun, Y.; et al. Sulfur-Rich Graphene Nanoboxes with Ultra-High Potassiation Capacity at Fast Charge: Storage Mechanisms and Device Performance. *ACS Nano* **2021**, *15* (1), 1652−1665.

(5) Baladés, N.; Sales, D. L.; Herrera, M.; Raya, A. M.; Hernández-Garrido, J. C.; López-Haro, M.; Molina, S. I.; et al. Exploring the Capability of HAADF-STEM Techniques to Characterize Graphene Distribution in Nanocomposites by Simulations. *J. Nanomater.* **2018**, *2018*, 4906746.

(6) Rubino, S.; Akhtar, S.; Leifer, K. A Simple Transmission Electron Microscopy Method for Fast Thickness Characterization of Suspended Graphene and Graphite Flakes. *Microsc. Microanal.* **2016**, *22* (1), 250−256.

(7) Hettler, S.; et al. Charging of carbon thin films in scanning and phase-plate transmission electron microscopy. *Ultramicroscopy* **2018**, *184*, 252−266.

(8) Nicholls, D.; Lee, J.; Amari, H.; Stevens, A. J.; Mehdi, B. L.; Browning, N. D. Minimising damage in high resolution scanning transmission electron microscope images of nanoscale structures and processes. *Nanoscale* **2020**, *12* (41), 21248−21254.

(9) Telychko, M.; et al. Sub-angstrom noninvasive imaging of atomic arrangement in 2D hybrid perovskites. *Sci. Adv.* **2022**, *8* (17), No. eabj0395.

(10) De Cecco, A.; et al. Non-Invasive Nanoscale Potentiometry and Ballistic Transport in Epigraphene Nanoribbons. *Nano Lett.* **2020**, *20* (5), 3786−3790.

(11) Datt Bhatt, M.; Kim, H.; Kim, G. Various defects in graphene: a review. *RSC Adv.* **2022**, *12* (33), 21520−21547.

(12) Huang, P. Y.; Ruiz-Vargas, C. S.; van der Zande, A. M.; Whitney, W. S.; Levendorf, M. P.; Kevek, J. W.; Garg, S.; Alden, J. S.; Hustedt, C. J.; et al. Grains and grain boundaries in single-layer graphene atomic patchwork quilts. *Nature* **2011**, *469* (7330), 389−392.

(13) Gong, Z.; Lai, X.; Miao, W.; Zhong, J.; Shi, Z.; Shen, H.; Liu, X.; Li, Q.; Yang, M.; Zhuang, J.; Du, Y. Br-Vacancies Induced Variable Ranging Hopping Conduction in High-Order Topological Insulator Bi4Br4. *Small Methods* **2024**, 2400517.

(14) Pham, V. D.; et al. Atomic-scale characterization of defects in oxygen plasma-treated graphene by scanning tunnelling microscopy. *Carbon* **2024**, *227*, 119260.

(15) Kang, H.; et al. Defect Identification of Nitrogen-Doped Graphene on Pt (111) Using Atomic Force Microscopy and Scanning Tunnelling Microscopy. *J. Phys. Chem. C* **2023**, *127* (42), 20742−20748.

(16) Ronci, F.; et al. High graphene permeability for room temperature silicon deposition: The role of defects. *Carbon* **2020**, *158*, 631−641.

(17) Kovalenko, S. L.; Andryushechkin, B. V.; Eltsov, K. N. STM study of oxygen intercalation at the graphene/Ni(111) interface. *Carbon* **2020**, *164*, 198−206.

(18) El-Ashquer, M.; Elsaka, B.; El-Fiky, G. On the Accuracy Assessment of the Latest Releases of GOCE Satellite-Based Geopotential Models with EGM2008 and Terrestrial GPS/Levelling and Gravity Data over Egypt. *Int. J. Geosci.* **2016**, 7 (11), 1323−1344.

(19) Pavlis, N. K.; Holmes, S. A.; Kenyon, S. C.; Factor, J. K. The development and evaluation of the Earth Gravitational Model 2008 (EGM2008). *J. Geophys Res. Solid Earth* **2012**, *117* (B4), B04406.

(20) Wahr, J.; Swenson, S.; Zlotnicki, V.; Velicogna, I. Time-variable gravity from GRACE: First results. *Geophys. Res. Lett.* **2004**, *31* (11), L11501.

(21) Deng, S.; Berry, V. Wrinkled, rippled and crumpled graphene: an overview of formation mechanism, electronic properties, and applications. *Mater. Today* **2016**, *19* (4), 197−212.

(22) Thomas, S. C. S. A method of producing a two-dimensional material, WO 2,017,029,470 A1, 2024 https://patents.google.com/patent/WO2017029470A1/zh-TW.

(23) Hartley, R.; Zisserman, A. *Multiple View Geometry in Computer Vision*, 2nd ed.; Cambridge university press2003.

(24) Nečas, D.; Klapetek, P. Gwyddion: an open-source software for SPM data analysis. *Open Phys.* **2012**, *10* (1), 181−188.

(25) Yang, G.; Li, L.; Lee, W. B.; Ng, M. C. Structure of graphene and its disorders: a review. *Sci. Technol. Adv. Mater.* **2018**, *19* (1), 613−648.

(26) Lin, Y.-P. *Functionalization of two-dimensional nanomaterials based on graphene* Aix Marseille Université, 2014.

(27) Salmeron, M. B. Selected Publications of Miquel B. Salmeron. *J. Phys. Chem. B* **2018**, *122* (2), 407−424.

(28) Wu, Q.; et al. Resolidified Chalcogen Precursors for High-Quality 2D Semiconductor Growth. *Angew. Chem., Int. Ed.* **2023**, *62* (29), No. e202301501.

(29) Wan, Y.; et al. Low-defect-density WS2 by hydroxide vapor phase deposition. *Nat. Commun.* **2022**, *13* (1), 4149.

https://doi.org/10.1021/acsomega.4c04675
ACS Omega 2024, 9, 43447−43452